Renewable Energy 246 (2025) 122828

Contents lists available at ScienceDirect

Renewable Energy

journal homepage: www.elsevier.com/locate/renene

Advances in the location and repairing of ribbon interruptions in photovoltaic modules

Félix G. Rosillo [a,*], Maria Beatriz Nieto-Morone [a], Richard Russell [b,1], Jesús Marín Muñoz [c], Juan Rodriguez Sánchez [c], Javier Yañez Gonzalez [c], María del Carmen Alonso-García [a]

[a] Departamento de Energía, Unidad de Energía Solar Fotovoltaica, CIEMAT, Av. Complutense, 40, 28040, Madrid, Spain
[b] BP Solar and Imec, Kapeldreef 75, B-3001, Leuven, Belgium
[c] División de Tecnología de Instrumentación Científica, CIEMAT, Av. Complutense 40, 28040, Madrid, Spain

ARTICLE INFO

Keywords:
Photovoltaic module
Repairing
Ribbon
Current detector
Compass
Defects characterization
End of life

ABSTRACT

One of the most frequent failures in PV modules is the total or partial interruption of ribbons that connect the cells in the module. In the case of modules with cells that have two ribbons on their surface, it is possible to distinguish between single interruptions (affecting only one ribbon of a cell) and twin interruptions (affecting both ribbons of a cell). In the case of repairing twin interruptions, it is possible to restore a significant part of the expected power, according to the nominal values of the module, which in modules with three diodes is in the order of a multiple of 1/3 of the nominal module power. In the case of repairing single interruptions, the recovered power reaches more modest values, up to 6 percentage points of the power prior to the repair. This article also shows the benefits to module fill factor depending on the repairs made and discusses metastable interruptions and the occurrence of new interruptions that can occur after initial repairs are made. A classification of single interruptions is proposed based on their type, and several methods to determine their location are described, highlighting one in particular for its simplicity and low cost. Finally, the relevance of carrying out a total repair (twin and single interruptions) or a partial repair (twin interruptions only) is discussed.

1. Introduction

The current environmental and ecological crisis is strongly linked to energy production. The development of Renewable Energy can help alleviate this crisis and photovoltaic solar energy (PSE) is in a privileged position to do this. Some components of photovoltaic modules are built from primary resources that are being depleted [1]. The circularity of PSE and increasing the useful life of its components is strategically important, both from the point of view of the generation of energy resources but also in the reduction of their environmental impact [2]. The repair of damaged photovoltaic modules could become a valuable contribution to the overall reduction of the environmental impact associated with photovoltaic solar energy [3].

It has been shown that second-hand photovoltaic panels can function satisfactorily after being repaired [4]. One of the most frequent breakdowns of photovoltaic modules, constituting around 10 % of the causes of failure is caused by an interruption(s) of the conductive strips located between two cells [5]. Locating the precise position of interruptions was described by K. Kato in Japanese and later translated into English and included in Ref. [5]. The location of single interruptions has been dealt with in Ref. [6]. The repair of this type of failure has been the subject of some attention [6,7] using relatively simple and potentially automatable repair methods. Other authors have evaluated the impact of this type of failure in modules manufactured specifically for this purpose [8,9].

A key aspect for repairing module interruptions must be the development of simple and low-cost techniques, so that there is an economic advantage of the repair compared to direct recycling, both in terms of the repair itself and the location of the interruptions [3,10].

In the previous publication [6] the location of both twin and single interruptions as well as the repair of twin interruptions were discussed in detail, but the repair of single interruptions was not addressed.

This article focuses on single interruptions, going into detail for various location techniques, focusing in particularly on electroluminescence. An economical, simple and precise method is presented for

* Corresponding author.
E-mail addresses: f.rosillo@ciemat.es (F.G. Rosillo), MariaBeatriz.Nieto@ciemat.es (M.B. Nieto-Morone), rick8419168@hotmail.com (R. Russell), jesus.marin@ciemat.es (J.M. Muñoz), juan.rodriguez@usual.es (J.R. Sánchez), yanezjavier2017@gmail.com (J.Y. Gonzalez), carmen.alonso@ciemat.es (M.C. Alonso-García).
[1] Independent Researcher.

https://doi.org/10.1016/j.renene.2025.122828
Received 26 November 2024; Received in revised form 4 March 2025; Accepted 6 March 2025
Available online 12 March 2025

locating simple interruptions. An additional localization method is presented that allows for the extraction of additional information, beyond mere location. A classification system for this type of fault is proposed, linked both to the time of its appearance and to its behavior and impact on the functionality of the photovoltaic module. Finally, the results of the repairs are analyzed, paying special attention to the advantage of repairing simple interruptions once twin interruptions have been repaired.

2. Methodology

2.1. Sample description

Four City Solar PQ 200, 2-ribbon modules were analyzed, which showed a reduction in power output. These modules have three diodes with nominal data of: maximum power 215 W, short-circuit current 7.9 A and open circuit voltage 37.1 V. The samples called M1 and M2 were used in the reference article [6] and the twin interruptions were repaired. For the present article, the single interruptions of these same modules were also repaired. Sample M3 of the cited reference was destroyed in a fall and could not be included in the present work. Two new samples are included instead, M4 and M5, which have been completely repaired for the development of the present work, first the twin interruptions and then the single interruptions. Samples M1, M2, M4 and M5 were chosen to represent different degrees of failure, at least as far as twin interruptions are concerned, based on the number of initially unusable cell strings. A module of the same make and model as the previous ones called M6 was reserved for the analysis of single interruptions that occur intermittently, and which we will hereafter call "metastable interruptions", since they appear and disappear depending on the module operating conditions, typically the temperature and the current flowing through the module.

2.2. Localization of interruptions and their repair

In [6] two types of interruptions were identified: Firstly, twin interruptions, which affect both ribbons that connect two cells and therefore cancel the operation of an entire cell strings in a module. Secondly, single interruptions, which affect only one of the ribbons that connect two cells. This fault does not cancel the operation of a cell strings, but does decreases the capacity of the module to generate electricity. We describe below the main localization methods that have been used in this work.

2.2.1. Detection of twin interruptions

The precise location of twin interruptions that affect the interconnection of two cells of a module requires the perforation of the backsheet of the module, since when the conduction of electricity by the affected cell string is cancelled, neither infrared images nor electroluminescence (EL) images show the cell string of cells affected by this type of fault. A cheap and simple process for locating twin interruptions and their repair was presented and discussed in Ref. [6]: Tone locators have been used, among others NIMO electronic TES011 and Fluke Networks PRO3000F50-KIT that inject an electrical signal of about 1000 kHz into the ribbons. The tone detector sensor emits an audible signal as long as there is electrical continuity in the ribbons. When this signal decreases or disappears, a twin interruption has been reached between two cells of the module.

2.2.2. Detection of single interruptions using electroluminescence

In [6] several methods for detecting single interruptions are described in detail. Among the sophisticated and high-cost methods are the taking of thermographic images or electroluminescence (EL) images. Low-cost methods that were used in the previous work include the measurement of the temperature of the module glass on the ribbons as well as the use of an alternating current detector with the module to be tested connected to a variac (autotransformer) powered by a conventional electrical network and optionally with a full-wave rectifier. A similar method using a current generator in combination with a current detector, used in photovoltaic arrays, was previously proposed and described in Japanese by K. Kato and later translated into English in an IEA report [5].

In [6], the possibility of locating the exact point of the interruption from electroluminescence images was questioned, when an area of the cell appears over-illuminated, while the rest of the cell appears dark. In these cases, it is not clear whether the interruption is at one end or the other of the dark area on the interrupted ribbon of the cell. In this work, we will proceed to analyze this statement in more detail, which after the analysis that will be presented, turns out not to be correct.

To find the characteristic signs of simple interruptions, electroluminescence images were performed, using the Raptor Owl 640 II EL camera with 640 x 512 pixels of 15 μm × 15 μm equipped with a Kowa LM25HC-VIS-SW 1″ 25 mm 12 MP VIS-SWIR lens. The modules were connected to a DELTA ELEKTRONIKA SM 70 V-22 A power supply, and currents of various values were supplied depending on the stage and purpose of the investigation, the values were generally close to the short-circuit current (I_{sc}).

To locate interruptions, the AC Voltage & Current detector brand EXTECH instruments and a compass were also used (this method will be described later in section 2.2.4). Using this information the simple interruption points were identified and related to the EL images.

2.2.3. Location of single interruptions using an electronic magnetic sensor

In this section we will describe the use of an easy-to-use magnetic field sensor that allows location of interruptions in real operating situations, when current is generated by the sun exposed module or with the module connected to a direct current power supply and in semi-dark conditions. Other authors have used magnetic devices similar to the one in this work with the purpose of finding defects in cells and in particular to detect interruptions in cell ribbons and interconnections [5, 11–13]. For this work, a device based on a Honeywell HMC1001 single-axis magnetic field sensor [14] was constructed. This sensor uses an Anisotropic Magnetoresistive (AMR), a technology based on the Wheatstone resistive bridge. Two characteristics of the sensor are its high sensitivity and relatively low cost. The magnetic field measured produces a potential difference in the branches of the bridge. The magnetic field to be detected corresponds essentially to a single spatial direction, permiting chosing a model which allows the measurement of the magnetic field along a single axis. The associated electronics are based on a scheme very similar to that described by the manufacturer [14], and consist of a circuit for the set/reset of the sensor and an operational amplifier for the voltage output signal, proportional to the potential difference produced by the effect of the magnetic field on the sensor. The output signal (in the range of a few volts) is sent directly to a conventional voltmeter or stored in a datalogger. To detect a simple interruption in the ribbons, the sensor is placed near or in contact with the module glass, moved over the cell ribbons and the output voltage is inspected. If an unusual reduction in the output voltage is recorded at an interconnection between two cells, it is considered that there is an interruption in that connection. The device allows for the acquisition of numerical data and for integration into an automated system for detecting simple interruptions. It can be operated at any angle of inclination of the module and presents some particularities regarding the effect of the direction of the current and the Earth's magnetic field. An East-West direction for the module ribbons is recommended and to choose the orientation of the sensor so that the signal from the Earth's magnetic field and the ribbon current magnetic field have the same direction and are therefore summed.

The device is powered by a 9V battery and can be used as a portable device in a real photovoltaic installation, when the modules are generating current by solar illumination. For the present work, in addition to the portable arrangement described above, the sensor has been used in

an arrangement that allows obtaining numerical data along the ribbons. Fig. 1 shows, on the left, the encapsulated device with its electronic circuit used in portable mode measuring the signal generated in the sensor on a ribbon of a photovoltaic module. On the right, the device is mounted on a frame supported on the same module, which allows manual movement on the XY axes. The XY frame consists of nichrome wire to measure the sensor position along each of the two axes. Measurements have also been made by manually moving the sensor along a single axis and using a scale graduated in cm as a reference. The procedure can be automated with different types of robots [11,12].

The output signal of the AMR sensor is in volts, although in this work we have chosen to convert it to current in amperes. The conversion of the voltage signal to amperes was done as follows: The sensor is placed over the section of ribbon lying between two adjacent cells. This ribbon must function correctly while its sister ribbon must be interrupted. Current is circulated through the module and therefore through the reference ribbon. The position of the sensor on the ribbon is adjusted to give the maximum output voltage signal. Next, the signal is taken from the sensor current circuit without current circulating through the module. This signal will correspond to the offset of the AMR sensor circuit and the Earth's magnetic field and will be subsequently subtracted to obtain the correct value in the output voltage/current ratio. Current is then passed through the module and its value is varied between 0 and the maximum current value to be measured. Once the Earth's magnetic field and the offset of the AMR sensor circuit have been subtracted, the measured voltage and current values are correlated. Fig. 2 shows the result of one of the measurements that relates the sensor output voltage to the current flowing through the ribbon. It shows excellent linearity between the voltage signal (from which the effect of the Earth's magnetic field has been subtracted) and the input current to the module. In the present configuration of the circuit connected to the AMR sensor, a saturation of the sensor occurs at about 4.6 A (or 5.79 V at the output of the sensor circuit). If necessary, this effect can be easily corrected by changing the gain of the amplifiers used with the AMR sensor or by moving the sensor slightly away from the ribbon (which is equivalent to decreasing the gain) and recalibrating. Alternatively, conversion of the AMR sensor voltage signal to current can be done by assigning zero current at the location of an interrupted ribbon and the value of the input current to the module on its sister ribbon. As in the previous case, these corrections would be applied to all points measured on both ribbons.

The calibration must be performed each time the sensor is moved using the displacement frame on the XY axes, since a bad centering of the sensor or a difference in the distance to the module glass can lead to erroneous results. Fig. 3 shows a diagram of the signal measurement device along the ribbon, using the XY frame equipped with nichrome

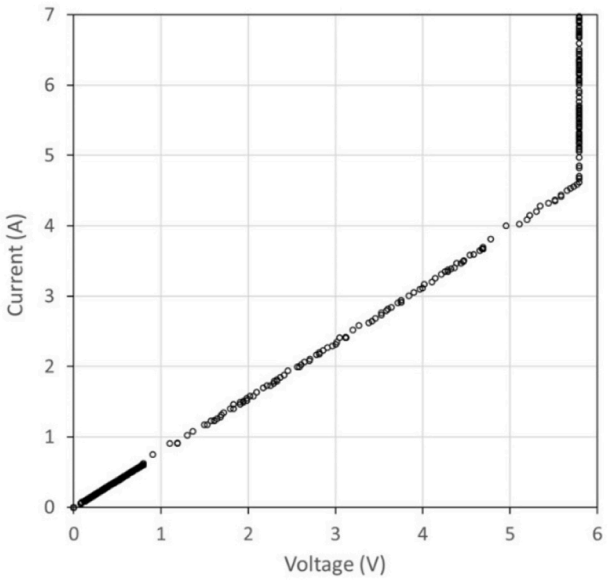

Fig. 2. Relationship between the current circulating in a module ribbon and the voltage supplied by the AMR sensor circuit (less magnetic field and offset). Saturation is observed at around 4.6 A.

wire to establish the position of the sensor during its movement, a module connected in semi-darkness to a DC power supply, a shunt for measuring the current flowing through the module and the AMR sensor. The resistance signals for calculating the position (nichrome wire), the current entering the module (through the voltage drop in a shunt) and the output voltage of the AMR sensor were stored using a Keysight 34972 A LXI data logger. Measurements were also made with a single guide axis and the aid of a graduated ruler (without nichrome wire), manually moving the sensor.

2.2.4. *Locating simple interruptions using a compass*

One of the purposes of this article is to present techniques for repairing photovoltaic modules which minimize the cost of the repair.

This section describes a method (Patent pending [15]) to locate simple interruptions between the solar cells of a module based on the Ørsted experiment [16] in which an electric current deviates the direction of a magnetic needle due to the magnetic field created by the current flowing in a conductor. This method is simpler, cheaper, reliable and equally fast or faster in addition to being easier to use than any of those described above. It does not cause damage to the back of the module, can be carried out in a real installation, with the only

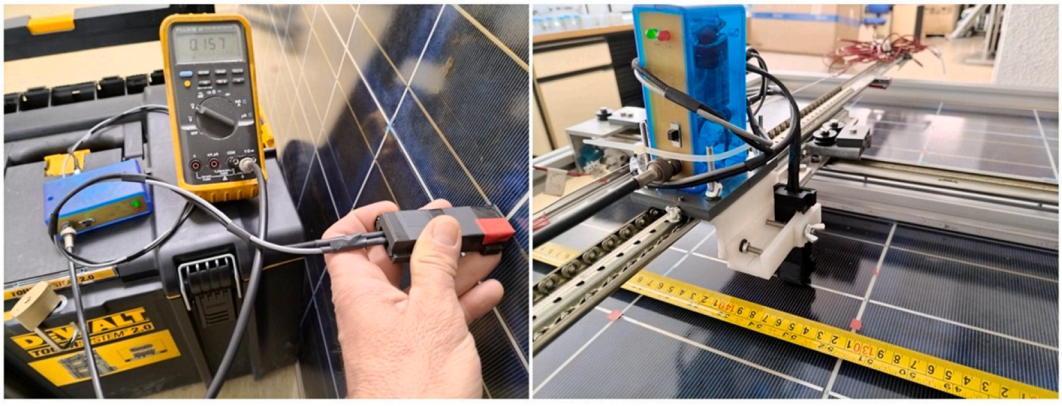

Fig. 1. On the left, the AMR sensor, its electronics and multimeter for recording the voltage output generated by the ribbon of a solar module, used as a portable device for detecting simple interruptions. On the right, the same sensor mounted on an XY frame with manual movement on the XY axes, placed on a solar module to record the magnetic signal along a ribbon of the module.

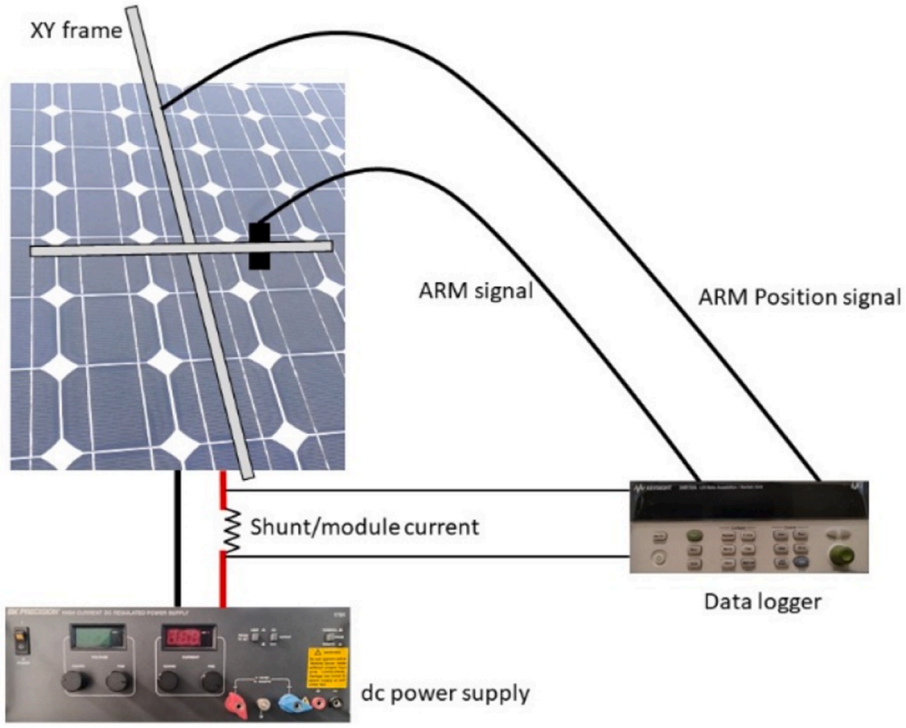

Fig. 3. System for measuring the current flowing through a ribbon of a photovoltaic module. It consists of an AMR sensor, positioned in an XY frame equipped with nichrome wire, a shunt for controlling the current flowing through the solar module, a power supply connected to the solar module and a data logger for data collection.

requirement that there is solar radiation and therefore current circulating through the ribbons of the module. It can also be put into practice indoors and in semi-darkness, using a continuous power supply connected to the module.

The method is based on detecting simple interruptions between the cells of a photovoltaic module using the magnetic field generated by the current that circulates through the conductive ribbons that interconnect the cells of the module. The magnetic field generated by the circulation of the current is reduced and finally ceases as the current approaches an interrupted ribbon indicating that, at that point, electrical conduction does not occur.

Fig. 4 illustrates the method with the module exposed to the sun and short-circuited (top), and with the module in semi-darkness (bottom) and connected to a power supply. The major axis of the module is oriented N-S in both cases. The magnetic needles the of compasses deviate due to the composite of the magnetic field generated by the current circulating through the ribbons and the Earth's magnetic field. Between the two ribbons of the module, the compasses are oriented with a difference of about 90°, (both in sunlight and in darkness) because in parallel cell strings the current flows in opposite directions. The module works as a source when exposed to sunlight and as a load when connected to a power supply in semi-darkness and therefore the current through each ribbon flows in opposite directions (ribbons on the left or right in Fig. 4).

The type of compass used can be basic, but should have a minimum quality. It is advisable to use a compass with liquid needle damping, of the type used in hiking or orienteering. For this work, Silva Classic model compasses were used, costing around €20.

It is recommended to locate interruptions with the module in a horizontal position and with the maximum possible current flowing. The limiting values for module inclination and current flowing through the module that still allow the method to be applied vary depending on the specific models of photovoltaic module and compass. For example, a magnetic needle mounted in a thick box may be little affected by the magnetic field generated by the current flowing through the ribbon. The application of the method requires the following steps.

1. Place the photovoltaic module in the sun or, if at dark, connected to a continuous power supply, preferably in a horizontal position.
2. Orient the module's major axis with the compass in a North-South direction or alternatively East-West (and subsequently West-East).
3. If the analysis is carried out indoors, connect the module to a power supply. If it is carried out in the sun, short circuit the module terminals or place a variable resistor between the terminals to dissipate the generated energy. It is preferable to work at current values close to the I_{sc}.
4. As explained in more detail in section 2.2.5, some interruptions only appear at currents close to the module's I_{sc} and after some time operating at this current: therefore it is recommended to perform an initial localization, as soon as the electric current flows through the module's ribbons and also a subsequent localization, after waiting at least 15 min and ensuring that during this time a current similar to the I_{sc} or the maximum power current circulates through the module. This makes it possible to locate ribbon interruptions that are activated under different operating conditions.
5. Place the compass on the module's glass, on one of the ribbons to be tested. In N-S orientation, at currents as low as 1 A it is already possible to detect the deviation (about 20°) of the compass' magnetic needle with respect to the axis to which the module has been oriented, but it is recommended to reach at least 2 A (with a deviation of about 30°). In the case of E-W and W-E orientation in a horizontal position, it is recommended not to go below 5 Amps (as long as the Isc of the module is not exceeded and depending on the model of the photovoltaic module and compass). To apply the method, in E-W and W-E orientations, the compass must point S-N: In the case of having the module oriented E-W and the compass pointing in a N-S direction when placed on the chosen ribbon, in order to test that ribbon, the module must be reorientated to the W-E axis and similarly with the W-E orientation, measuring half of the ribbons in the E-W orientation and the other half in the W-E orientation.

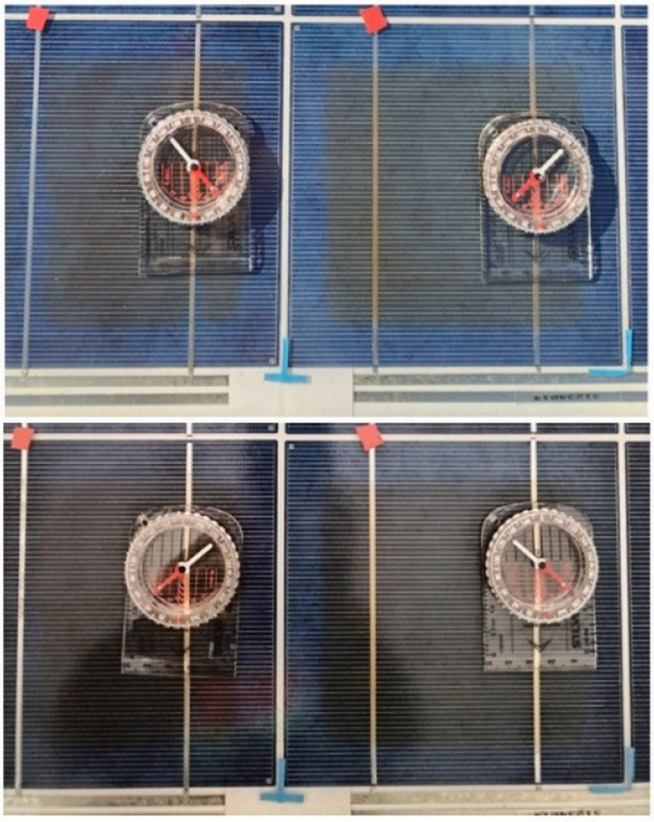

Fig. 4. Above, module operating normally exposed to the sun. Below, module powered in semi-darkness by a 7 A DC source. In both cases, two compasses have been placed on ribbons of adjacent cells which have opposite directions of current flow. When comparing the photos, it can be seen that the compasses have their magnetic needles oriented in opposite directions according to the direction of the current. The orientation of the ribbons is N-S in both cases.

6. Move the needle along the module ribbons paying special attention to over the section of ribbon lying between two adjacent cells. It is also possible to do the test by placing the compass directly on each of the cell junctions.
7. With the module orientated N-S (and also E-W or W-E), if at one of the connection points between two cells it is observed that the compass returns to the N-S orientation, at that point the current is interrupted and therefore a fault has been detected.

Fig. 5 shows various compass positions on the ribbons. North has been shown pointing to the bottom of the page. The black portions of the magnetic needles of the compasses shown in the figure correspond to magnetic North. In the ribbon marked 1.a) the compass is shown at three points on a ribbon: above on one cell, below on another cell and in the centre on the intercell connection. It can be seen that the compass needle shows a deviation from the north-south axis due to the presence of the magnetic field generated by the current conducted by the ribbons. In the case shown the needle deviates from the N-S axis in a N-W direction. In the series of adjacent cells, the deviation from the N-S axis will be N-E and at a similar angle. This fact will not affect the analysis and is due to the fact that, due to the accordion packing of the series of cells within a photovoltaic module, the current flows in the opposite direction to that of the ribbon described in the example. Since in ribbon 1.a) there is no difference in the orientation of the compass in any of the three positions represented, it follows that there is no intercellular interruption in that ribbon.

In ribbon 1.b) the sister ribbon of the same cell, the opposite case is shown: While the deviation of the compass is similar in the positions on the cells, in the central position on the interconnection of the cells, the magnetic needle is oriented North-South. In this case, an interruption of the electrical connection between the two cells has been detected, which can be repaired. This detection is due to the fact that, when the current is stopped conducting, the magnetic field generated by that current disappears and the compass tends to orient itself in its natural direction, according to the Earth's magnetic field.

The same analysis can be performed by alternately orienting the module in the E-W and W-E directions. This orientation is more sensitive than the N-S orientation, but at the cost of having to reorientate the module to test both current directions, in order to analyze half of the PV

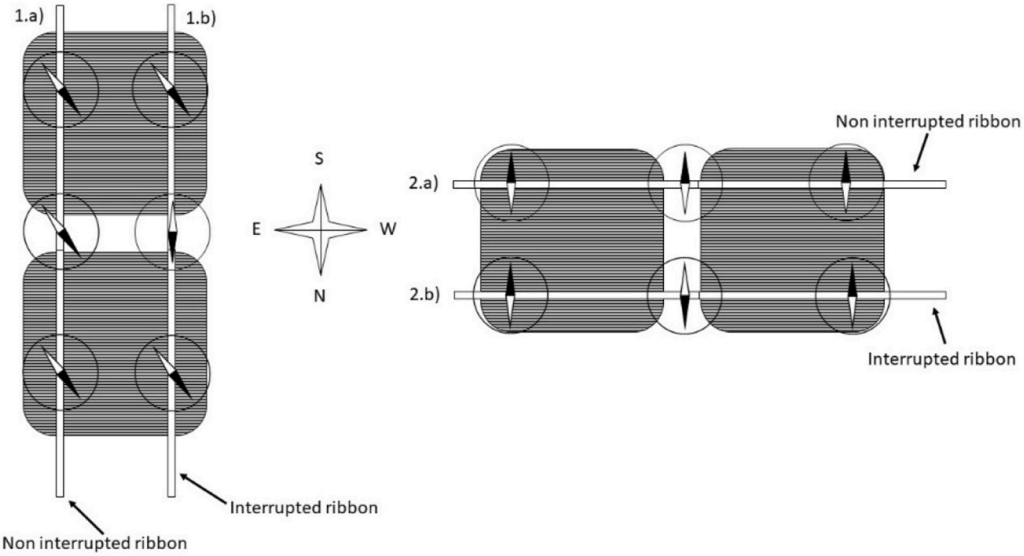

Fig. 5. Two solar cells with their ribbons oriented N-S (left) and E-W (right), and current-sensing compasses. The ribbon marked as 1.a) and N-S orientation represents the case of two cells without interruption in that ribbon. The ribbon marked as 1.b) and N-S orientation represents the case of two cells with interruption in the ribbon tested, at the point where both cells should be connected. The ribbon marked as 2.a) and E-W orientation represents the case of two cells without interruption in the ribbon tested. The ribbon marked as 2.b) and E-W orientation represents the case of two cells with interruption in the ribbon tested, at the point where both cells should be connected. In this last case the needle returns to its natural position due to the Earth's magnetic field.

module ribbons each time. Fig. 5 shows the use of the E-W orientation. In the uninterrupted parts of ribbons 2.a) and 2.b) and due to the magnetic field created by the current, the magnetic needle of the compass is oriented in the S-N direction, opposite to that of the Earth's magnetic field. On the contrary, the magnetic needle in the centre of ribbon 2.b) has been reorientated in the N-S direction, revealing that the electric current has disappeared, as the magnetic needle has returned to its natural direction, thus interrupting the conduction of current at that point on ribbon 2.b). To detect interruptions in the neighboring series where the electric current flows in the opposite direction, the panel must be reorientated in the W-E direction, otherwise the needle will always point north, making it impossible to detect any interruption.

Regarding the compass to be used, it should be taken into account that if the box in which the magnetic needle is mounted on is very thick, the needle will move away from the ribbons but the deviation effect is reduced as the magnetic field they generate is inversely proportional to the distance. Likewise, the degree of deviation of the compass depends on the value of the current that circulates through the ribbons.

It is possible to apply a method similar to the one proposed using a mobile phone, provided that it incorporates a magnetic field sensor and a "compass" application is used. To do this, the most sensitive point to the magnetic field on the surface of the phone must be located. Using a mobile phone requires prior characterization work that may differ between each phone model and its compass application.

2.2.5. *Analysis of simple metastable interruptions*

During this work, the presence of simple interruptions was observed, which appeared and disappeared in an apparently random manner, but showing some relationship with the module temperature, with the operating time of the module (as a load or as a source) and with the value of the current circulating through the module. We will call these types of interruptions from now on metastable simple interruptions. To locate this type of interruption we have used almost all of the described techniques for locating simple interruptions (EL images, compass and current locators) with the module connected to a power source or exposed to the sun, varying the current that circulates through the module and the circulation time of the current.

2.3. *Repair of interruptions and appearance of new interruptions*

The article [6] details the process of repairing interruptions, identical to that used in this article, both for single interruptions and for twin interruptions. It has been observed that the repair of simple interruptions can be followed by the appearance of new simple interruptions. This leads to the need to repeat the processes of locating simple interruptions after repairing each set of interruptions initially found. In this sense, to locate all simple interruptions, it is important to keep a current similar to the I_{sc} or at maximum power circulating through the module for at least 15 min.

3. Results and discussion

3.1. *Location and analysis of simple interruptions using an electronic magnetic sensor*

The AMR sensor allows the location of simple interruptions in a portable or laboratory-based manner, with the module operating in semi-darkness connected to a power supply or in a real installation with the module operating normally in the sun. Although the simplest detection of interruptions consists of observing significant changes in the output signal of the sensor when moving it over the ribbons and noting the interruption points, in the following we will illustrate its operation in more detail and graphically. To do this, the methods described in section 2.2.3 and in Fig. 3 were used and compared with the EL measurement.

Fig. 6 presents the measurements of the current flowing through the two ribbons of a series of 10 cells of the M6 module. It was previously known that one of the ribbons had two single interruptions, which are represented by red circles in Fig. 6. This was confirmed using the other localization techniques described (compass, AC localiser and EL). To perform the measurements presented in the figure, a current of approximately 5 A dc was passed through the series of cells and the current along the two ribbons was estimated using the AMR sensor applied to the front of the module and the methodology described in section 2.2.3. It can be observed that the sum of the currents flowing through the two ribbons approximately coincides with the current injected into the cell. In the vicinity of the interruptions, the current flowing through the interrupted ribbon decreases until it is zero (blue curve), while in its sister ribbon (brown curve), in perfect working condition, the current increases until it is close to 5 A. The variation in the current in the ribbons of the cells in the vicinity of the faults affects the entire length of the ribbons in the two cells surrounding the interruption. That is, there is no sudden interruption of the current in the vicinity of the interruption (for example, cells 1 and 2 in Fig. 6), but the current in the ribbons begins to increase/decrease gradually, practically at the junctions of the cells before/after the interruption (cell 3 in Fig. 6).

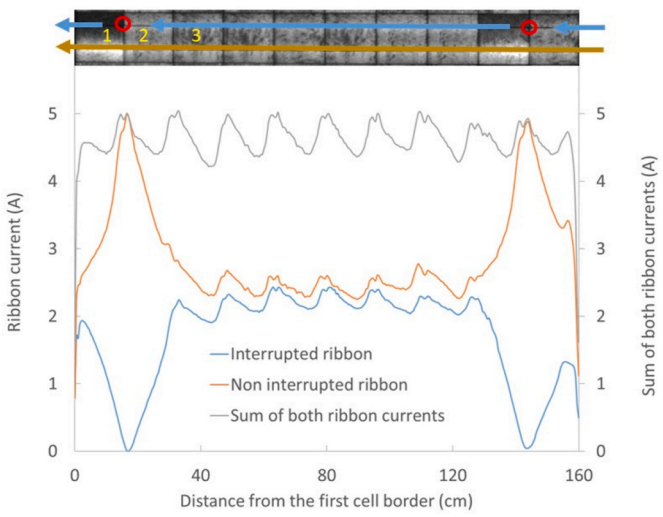

Fig. 6. Current measured on the parallel ribbons of the same series of cells of the M6 photovoltaic module powered in semi-darkness at 5 A and their sum. One of the ribbons (blue) shows two single interruptions at the positions indicated by red circles in the superimposed EL image and which have been matched with the corresponding peaks and valleys of the current curves. The coloured arrows on the EL image represent the direction of electron flow in the ribbons. (For interpretation of the references to colour in this figure legend, the reader is referred to the Web version of this article.)

Regarding the oscillations of the current curves in Fig. 6, there is a complete correspondence between the peaks and valleys of the curves and the junction points of the ribbons between the cells. In general, it is observed that the current carried by a ribbon decreases in the direction of the electron flow and at a third of the distance from the edge of the cell, it begins to increase until it reaches its maximum value. The analysis of these observations is outside of the purpose of this article, but it provides interesting information on the dynamics of surface currents in photovoltaic cells and coincides with what has been observed by other authors [17].

The use of the AMR magnetic sensor with the module acting as a current generator and taking measurements on the surface of two cells is illustrated in Fig. 7. In this case, the module was exposed to the sun, and the generated current was adjusted to approximately 1 A by orienting the module with respect to the sun and using a variable resistor. The reason for this current limitation is that, in order not to cast shadows on the module, the measurement was carried out by moving the AMR sensor over the surface of the backsheet, not on the front, as in the

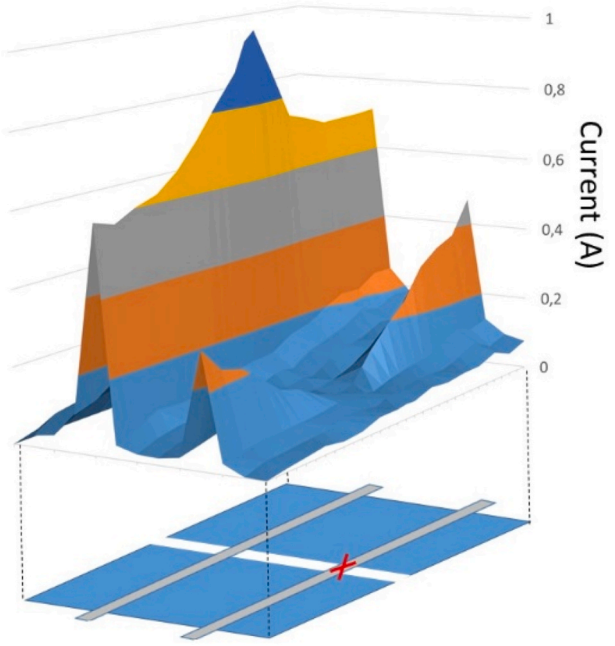

Fig. 7. Current measured on the surface of two cells of the M6 module exposed to the Sun and generating approximately 1 A. Below, a diagram of the two cells is shown. Each point on that surface corresponds to the current shown on the z axis of the figure. The interruption of one of the ribbons is illustrated with a red cross. (For interpretation of the references to colour in this figure legend, the reader is referred to the Web version of this article.)

previous example. The module was oriented so that the direction of maximum sensitivity of the AMR sensor coincided with that of the module ribbons. Since there is no glass on the back of the module, the distance between the sensor and the cell surface was much smaller than in the previous case and it was necessary to limit the current flowing through the module to avoid saturation of the sensor. Fig. 7 shows the current flowing through the surface of two cells that have one of their ribbons interrupted, as well as an idealized image of the two cells and the interruption of one of the ribbons.

Approximately 200 measurements were made distributed on the rear surface of the two cells. As shown in Fig. 6, it was observed that the current not collected by the interrupted ribbon is collected by the uninterrupted ribbon. Since the AMR sensor model used is sensitive on a single axis, the current is recorded in only one direction. That is, there may be net currents in alternative directions that are not reflected in Fig. 6 [17] but they would not affect the purpose of this work. The measurement of the module in semi-darkness and connected to a power supply shows similar results.

This technique allows mapping of the current that circulates through the surface of the cells. In addition to detecting ribbon interruptions, it allows the detection of other phenomena (such as the decrease and increase of the current along the ribbons and on the surface of the cells) and which have been treated in detail in other works ([18–20]).

3.2. *Localization of simple interruptions using electroluminescence. Comparison with current locator and compass*

Fig. 8 shows the electroluminescence image of the M6 module, connected as a load to a DC power supply and which presents eleven single interruptions. The yellow line that joins the positive and negative poles of the module represents the idealized path of the current in each cell, while the red arrows indicate the direction of the propagation of the electrons.

Since in this arrangement the module works as a load, the current flows from the positive to the negative pole and therefore the electrons flow from the negative to the positive pole. The light blue boxes indicate areas close to the ribbons of each of the eleven cells with single interruptions, which receive electrons generated by the power supply and whose characteristic feature is to present a greater brightness than its sister ribbon, which barely conducts current (as described for single interruptions in Fig. 6). Meanwhile, the sister ribbon of the same cells remains dark due to the reduction or interruption of the circulating current. The red circles represent the interruptions previously located by

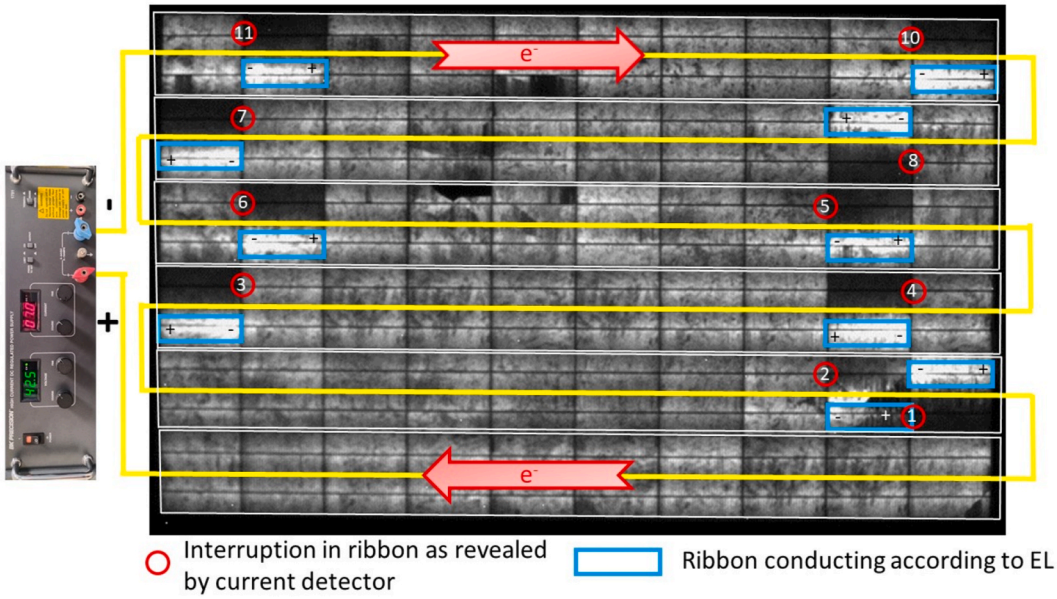

Fig. 8. EL image of the M6 module in semi-darkness, connected to a DC power supply, represented on the left. The polarity is indicated in the connection box (+ and -). The path followed by the currents in the series cells of the module is schematized by yellow lines. The eleven single interruption points as found with the current locators and the compass are indicated in red numbered circles. Blue outlined boxes highlight the conducting ribbons in cells with single interruptions. The conducting ribbons with an interrupted sister ribbon show a higher brightness than other areas of the cells. In these cells their polarity is indicated with the signs + and -. The direction of electron flow has been represented by thick arrows. (For interpretation of the references to colour in this figure legend, the reader is referred to the Web version of this article.)

means of the current and compass detectors. In the case of the EXTECH AC Voltage & Current detector, since it is only useful for detecting alternating current, the module was connected to the network by inserting a variac (Variable autotransformer) and a full-wave rectifier, adjusting the voltage and current to the desired values [6]. With this latest setup and due to the presence of the full-wave rectifier (and therefore a single direction of the current) the compass works correctly and complete coincidence of the results obtained could be verified.

From the analysis of the EL in Fig. 8 and the result of the analysis with a current locator and compass, it can be deduced that, taking an EL image as a reference, the interruptions are located in the dark ribbon next (sister) to an illuminated ribbon and in the part closest to the negative pole of the connection box (or of the cell itself). It has been verified that this is valid for all the modules analyzed in this work.

Fig. 9 presents an idealized three-dimensional diagram of the physical phenomena described, in the case of connecting the module to a power supply in semi-darkness. The direction of electron flow is from cell A to cell C. The interruption appears on ribbon 1A between cells A and B. The electrons then move to ribbon 2A, which is not interrupted. The consequence is that ribbon 2B receives almost all of the current flowing through the module and therefore more electrons than without a neighboring interruption and, by emitting more radiation than normal, appears very illuminated in the EL. On the other hand, the interrupted ribbon (Ribbon 1B) does not receive electrons and appears dark in the EL image.

If the module is placed in the sun, it works as a generator and Fig. 9 would be valid by simply reversing the direction of the arrows that represent the movement of the electrons. To clarify this, the two situations have been represented in Fig. 10 in a two-dimensional scheme, with the cells functioning as a source (below) and as a load (above). With the module in the sun, functioning as a source (below), electrons will flow from cell B to cell A. With the module in semi-darkness, functioning as a load (above) connected to a continuous power supply, electrons will flow from cell A to cell B. Measurements made with the AMR current-detecting device indicate that while these statements are strictly true very close to the ribbon interruption, the current received by the broken ribbon begins to decrease/increase as we move away on both sides of the interruption (Fig. 6). Finally, placing two compasses on the ribbons in darkness and in light shows this situation very graphically, as the magnetic needle is oriented in different directions depending on the direction of the current and its intensity (see Fig. 4).

3.3. Metastable interruptions

Some single interruptions show a metastable character, that is, an interruption can appear and stop appearing on a ribbon depending on the value of the current flowing, the temperature of the module, or the time the current is circulating.

Fig. 11 shows the EL images of four cells of the M6 module, where the presence of metastable interruptions was suspected. EL images were taken with different values of current flowing through the module. It can be observed that at 2 A two over-illuminated ribbons have appeared, indicating the presence of two simple interruptions. When going from 3 A to 4 A, one of the interruptions passes to the opposite ribbon of the same cell to disappear at 7 A and finally reappears when the module is kept at 7 A for 40 min.

From a practical point of view and for the purpose of repairing modules, the observation made advises to determine the localization of interruptions at medium current (for example 3 A) and at currents close to the I_{sc}. Additionally, it is advisable to carry out the localization in both cases immediately after establishing each current value and as a guide, 15 min after keeping the module at each of the current values. In future work, a more detailed characterization of the behavior of the metastable interruptions will be carried out.

3.4. Types of interruptions located and definition of typology for single interruptions

To locate the single interruptions in the four modules of this work, EL images were used to a limited extent and current locator and compass techniques were used extensively. These last two methods are more agile, being able to find interruptions almost immediately. Another advantage of these two methods compared to the EL technique is that their ease of implementation allows the interruption searches to be easily repeated as many times as necessary, useful after a repair (which, as we will see below, can be followed by the appearance of new

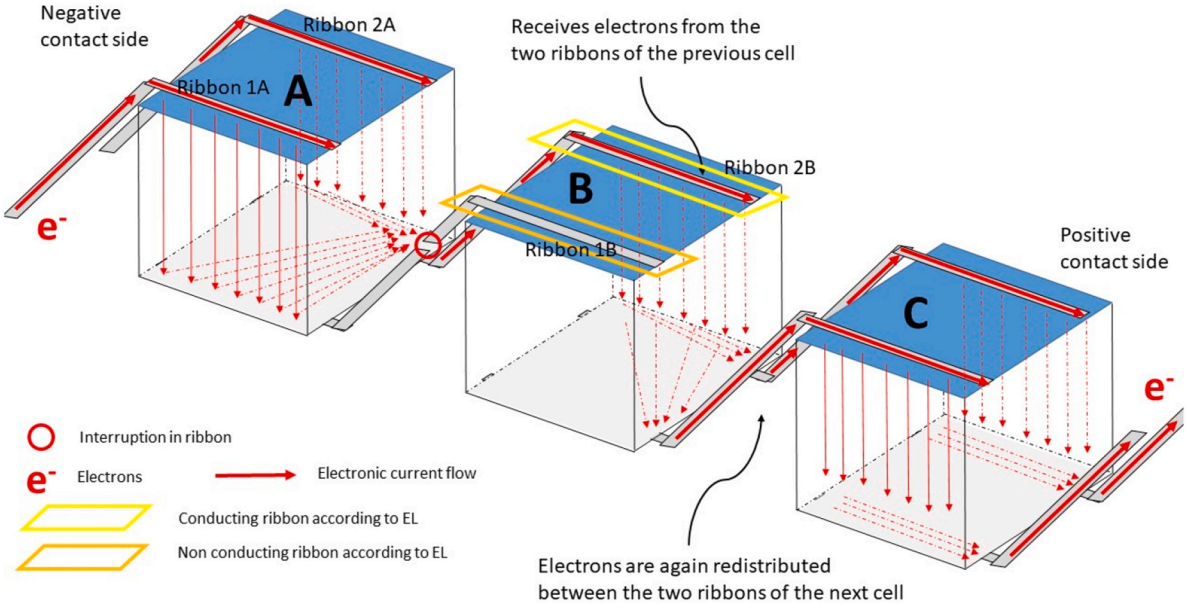

Fig. 9. Schematic representation of the operation of three cells in series fed by a power supply in semi-darkness and with an interrupted ribbon, between cells A and B. Cell C works normally. In cell A the electrons move towards ribbon 2B of cell B which is not interrupted. The trajectories and density of the red arrows representing the flow of electrons are merely illustrative. (For interpretation of the references to colour in this figure legend, the reader is referred to the Web version of this article.)

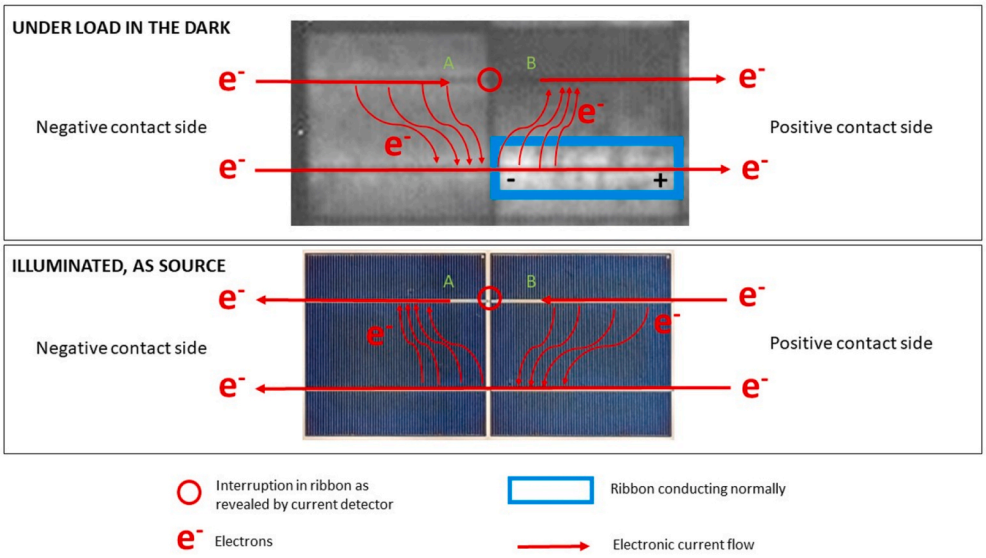

Fig. 10. Representation of the flow of electrons between two cells with a single interruption, with the module functioning as a load (top) connected to a power supply (EL image) and functioning as a source (bottom) visible image and exposed to the sun.

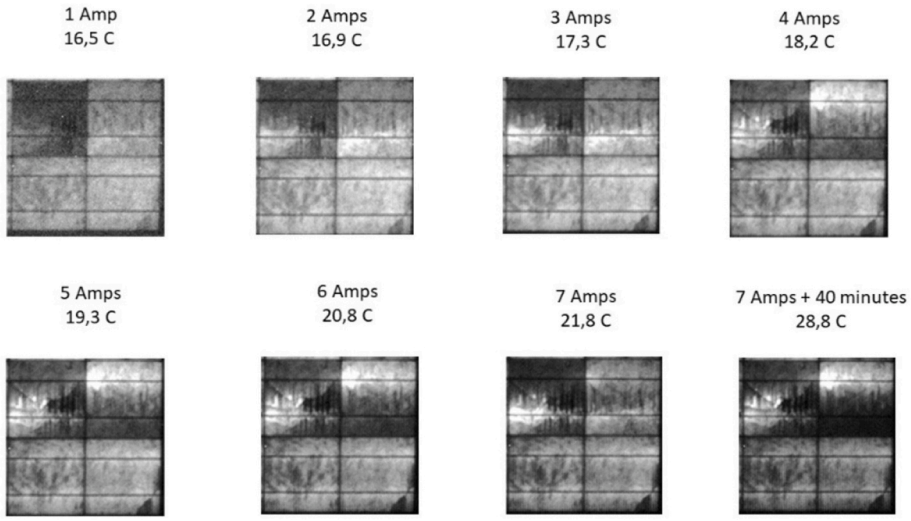

Fig. 11. Electroluminescence images of four cells of the M6 module, taken at different values of the current flowing through the module. Between two and 3 min elapsed between the acquisition of each image. The last image was acquired 40 min after the previous image.

interruptions) and especially with metastable interruptions described in the previous section. We will use EL images mainly as a basis for the figures that illustrate the following sections and because they allow us to graphically show the progress of the repair.

It has been observed that, in metastable interruptions, the sister ribbon of the same cell may appear interrupted alternately, and depending on the value of the current flowing, the temperature or the elapsed time, one or the other of the connections between two cells may be interrupted (section 3.3). Another effect observed is that the repair of an interrupted single ribbon is followed, in approximately half of the cases, by the interruption of the sister ribbon of the same cell. These two situations described may occur, eventually in the same cell, that is, a cell may show single interruptions that are both metastable (may or may not appear) and alternating (may affect one intercellular connection or another).

Based on these findings and in order to facilitate subsequent analysis, the interruptions found during this work have been classified into the following categories.

- Twin interruption: It affect both connections between two cells of the module, disconnecting a complete cell string. In the case of the analyzed modules with two ribbons per cell, the interrupted series represent multiples of 1/3 of the number of cells and therefore a significant loss of power for the module. In the case of cells with a greater number of ribbons, two interruptions may not mean the interruption of an entire cell string, as described in Refs. [8,9].
- Single interruption: It affects one of the junctions between two cells of the module, generating a moderate loss of power.
- Delayed single interruption: Single interruptions that appear after repairing the single interruptions described above. In most cases they appear after repairing their failed sister single junction. In some cases, they appear in cells that did not show initial single interruptions and only appear after repairing the single interruptions initially detected in the module (module M5 in Fig. 12).
- Delayed twin interruption: Interruption formed by a single interruption and a delayed single interruption. It is a descriptive concept, since both single connections are interrupted at different times, not at the same time.

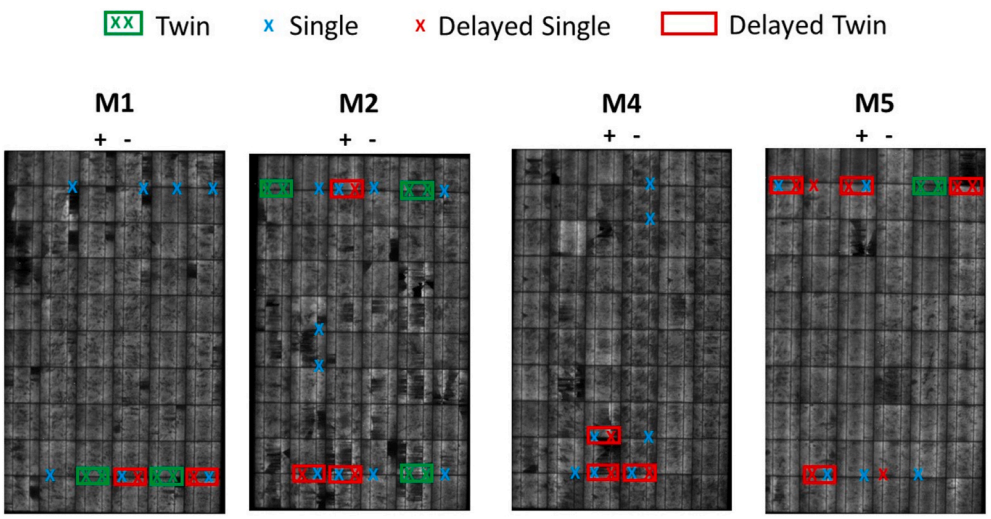

Fig. 12. Interruptions found and repaired in the modules. The original twin interruptions, two types of single interruptions (single and delayed single) and an additional type of twin interruption (delayed twin) are represented. The interruptions have been represented on the EL image of each of the modules at the end of the repair process.

It could be thought that the special case of delayed single interruptions that appear in ribbons whose sister ribbon has not been repaired and therefore do not generate delayed twin interruptions, could correspond to single interruptions not initially detected. However, because in each module the detection processes were carried out by different techniques and repeatedly before each repair process, we discard this possibility and consider that these interruptions are due either to metastable interruptions that become stable interruptions after the initial repair or to interruptions generated, by an unknown mechanism, as a result of the repairs carried out.

Fig. 12 graphically presents the module interruptions found and repaired, superimposed on the EL image obtained at the end of all repairs made. The repairs were carried out as described in Ref. [6]: Locating the interruption, suppressing backsheet using handicraft tools like mini rotary drill tools and accessories, particularly grit sanding band, inserting and soldering a piece of ribbon complements and finally sealing with special silicone. The typology of repaired interruptions is also detailed, as defined previously. As a special case, in the upper right part of module M5 in Fig. 12 a delayed twin interruption composed of two delayed single interruptions is shown: This is because in this case both single interruptions were metastable, that is, they appeared in an apparently random and alternating manner, after the rest of the repairs had been carried out. For simplicity, we have preferred not to introduce a new category. In this same module, the two delayed single interruptions appeared in cells that had not initially shown any interruption.

Table 1 presents the number of interruptions in the set of the four modules analyzed, which correspond to each of the four categories described. The first column specifies the module reference, the second column presents the number of cell string initially interrupted by twin interruptions in each module and which are equivalent to two interrupted ribbons in the same cell. The third column presents the number of initial twin interruptions.

Comparing with the previous column and with Fig. 12 it can be observed that module M2 presented two twin interruptions in the same cell string. In this case, the repair of an initial twin interruption was followed by the immediate appearance and repair of an additional twin interruption, which had not been recorded before that repair. The fourth and fifth columns show the number of single interruptions and the delayed single interruptions, respectively. The sixth column shows the number of delayed twin interruptions that occurred between the same cells that previously showed single interruptions.

Of the 15 delayed single interruptions, two of them did not constitute a delayed twin interruption (M5) and two others affected the same cell, leaving 11 that generated delayed twin interruptions. That is, 38 % of the initial single interruptions (29 breaks) end up forming part of delayed twin interruptions. This high number of single interruptions that end up becoming twin interruption points to a progressive degradation of the connections between cells that could be at the origin of the twin interruptions. We conclude that it may be reasonable that once an initial single interruption is detected, the two connections present between the two cells should be repaired, without waiting for the non-faulty ribbon to become interrupted soon afterwards. In this work, this was not done, since it was preferred to repair only the single interruptions that were evident in order to, in a future work, study in detail under operating conditions how these single interruptions are reproduced (or not).

The seventh column of Table 1 shows the total number (56) of

Table 1
In the first column, the module reference; in the second column, the number of complete cell string initially interrupted; in the third to sixth columns, the number of interruptions of each type, as defined in the text. The last column shows the total number of interruptions repaired in each module, regardless of their typology.

Module	Cell strings initially interrupted	Twin interruptions/(Ribbons interrupted)	Single interruptions	Delayed single interruption	Delayed twin interruption	Interruptions repaired
M1	2	2/(4)	7	2	2	13
M2	2	3/(6)	10	3	2	19
M4	0	0/(0)	7	3	3	10
M5	1	1/(2)	5	7	4[a]	14
TOTAL	6	6/(12)	29	15[b]	11	56

[a] Includes the case of a twin interruption that appeared delayed without relation to any delayed single interruption.
[b] Two of them do not generate a twin interruption and two others constitute a new delayed twin interruption.

ribbons repaired. Considering that each module has 60 cells and therefore 120 intercell connections and that 4 modules have been repaired, the percentage of failed and subsequently repaired junctions amounts to 12 % of the intercell connections.

The interruptions shown in Fig. 12 show a clear preference for intercell connections located towards the top and bottom of the major axis of the modules failing, with some exceptions in modules M2 and M4. It is noteworthy that in no case were there interruptions between cells at the module ends, where the wires change direction. We found a similar behavior in two other modules from other manufacturers (Scheuten Solar Multi 200 PS and Conergy PowerPLus 220P). We currently have no explanation for these facts.

3.5. Power recovery, FF and module functionality

Although one of the objectives of this paper is to demonstrate the use of simple techniques for locating single interruptions - i.e. the current locator and the compass - it is instructive to observe the evolution of EL images in the successive steps of the repair. La Fig. 13 presents three stages of repair of the photovoltaic modules. First, EL images of the modules before any intervention. Second, the images after repairing the twin interruptions and finally, in the third column of images after repairing all the single interruptions found (including delayed interruptions). Intermediate ELs showing delayed single interruptions were not performed, due to the need to speed up and reduce the effort invested in carrying out the repairs.

Figs. 13 and 12 show the location of all the repaired interruptions and their types. The M4 module is characterized by not having shown initial twin interruptions. The first column of EL images shows how an attempt was made to select modules with different degrees of failure: 2/3 of the cell strings initially failed in the case of samples M1 and M2 and with the cell strings active in different places, 1/3 of the cell string initially failed in the case of module M5 and no cell strings initially cancelled in the case of sample M4. In Fig. 13 and from left to right, the reduction of clear areas associated with their interrupted ribbon is evident, which confirms that the single interruptions found have been repaired, an observation confirmed with the compass and the current locator.

Fig. 14 presents the IV curves resulting from the two repair phases of the four modules: before repair, after repairing the twin interruptions

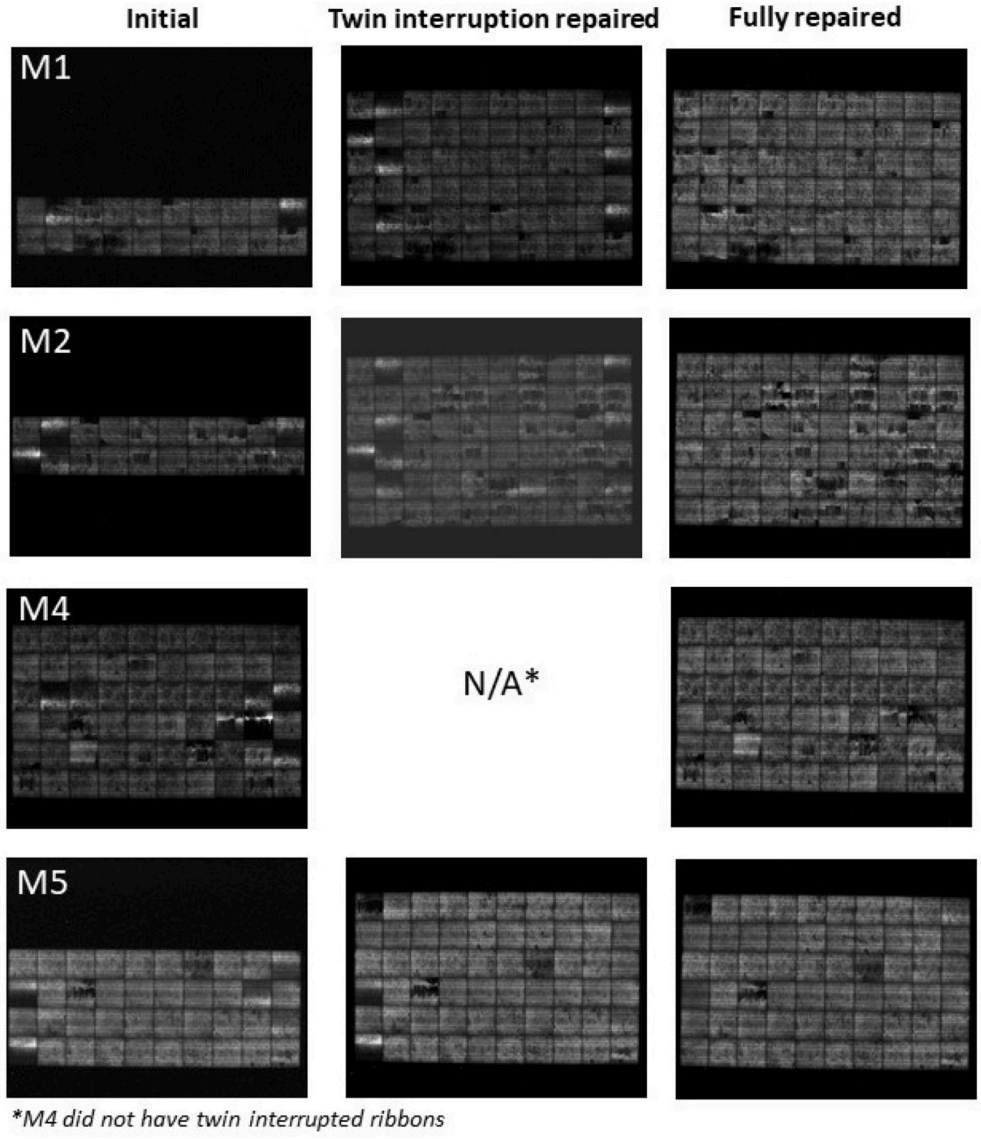

Fig. 13. Electroluminescence images taken of each of the four modules, showing their initial state before any repairs (left), their appearance after repairing the twin interruptions (center) and finally their final state after repairing all interruptions, single and twin. The M4 module lacked twin interruptions and therefore the central EL is missing.

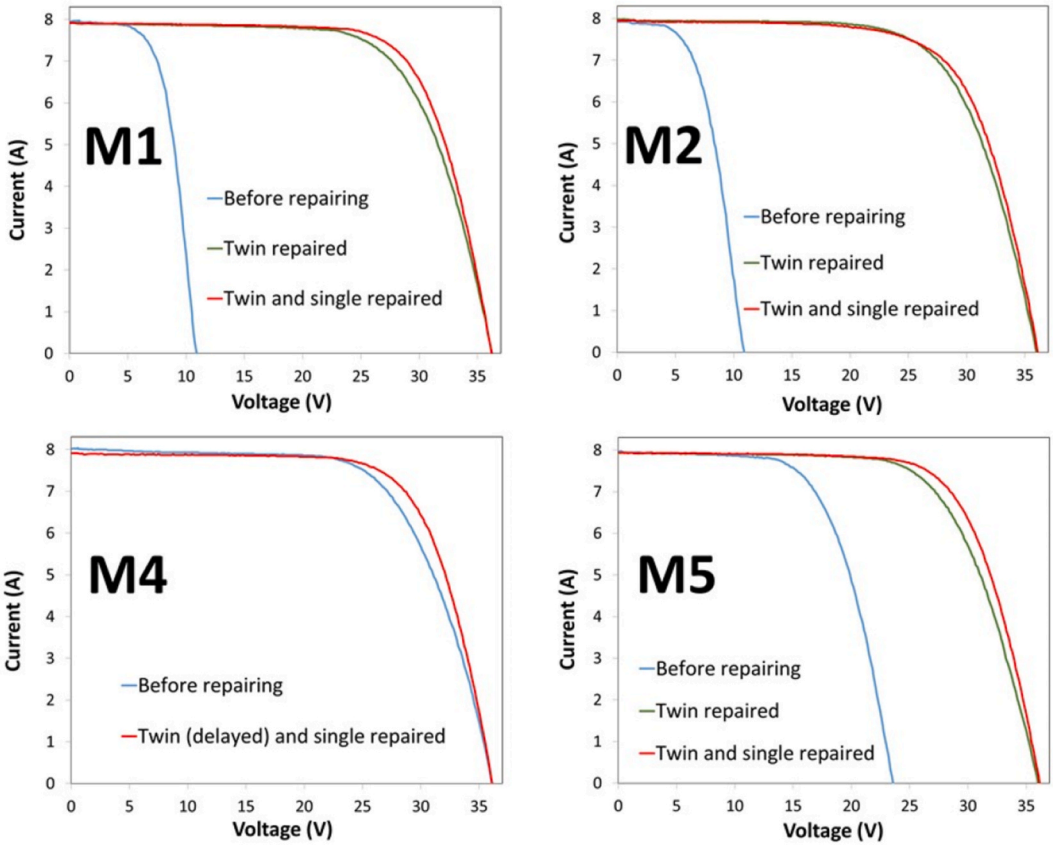

Fig. 14. IV curves at STC of the four modules before repair, after repairing the twin interruptions (except in the case of module M4 which had no such interruptions) and when the repair was completely finished.

and when the repairs were completely finished. It can be observed that, as shown by the EL images or with open circuit voltmeter measurements, in modules M1 and M2 the generation of electricity by two thirds of the cells had been lost, module M5 showed an initial loss of one third of the cells and module M4 suffered a much more moderate loss, but evident in the IV curve, compared to the values reached after the repairs.

Regarding the recovery of the power generated by the modules, which is the main objective of this work, Table 2 presents the measured values of the maximum module power in STC initially without repair, after having repaired the initial twin interruptions and finally after completely repairing each of the modules. The percentage of power gain when passing from the phase without repair to the phase with twin interruption repair (which we call phase 1) and the percentage of power gain from the twin interruption repair phase to the full repair phase (which we call phase 2) are also presented. It is observed that the first phase, corresponding to the repair of twin interruptions, very large power gains were obtained, reaching a four-fold increase in the power produced, with respect to the initial value without repair, as already pointed out in Ref. [6]. The second phase, consisting of the repair of single interruptions, involves more modest power increases, ranging from 2 % to 6 % with respect to the previous phase. Although the gains are not high, they are not negligible. The seventh column shows the power gain of the complete repair process.

If Table 2 of this work is compared with Table 2 of reference [6] shows different values for the powers recorded before repairing and after repairing the twin interruptions. This is due to a data transcription error that was made during the preparation of Table 2 in Ref. [6]. The conclusions do not change for the previous article and Table 2 of this article has been repeatedly checked to avoid the error made in the previous article.

The fill factor (FF), i.e. the maximum power divided by the product of $I_{sc}$and open circuit voltage is a figure of merit often used to compare the technological quality of different photovoltaic modules. In this work, although we consider power recovery (Table 2) to be the most important parameter, in Table 3 we reflect the evolution of the FF in each of the repair phases of the four modules. In this case we use the FF as a parameter to measure the evolution of each of the modules analyzed, and its improvement after each repair.

The nominal FF value of these modules is 0.73. In the FF table it can be seen that before the repair they had fallen to values as low as 0.55 and

Table 2
Maximum STC powers measured before repair, after repairing the twin interruptions and after repairing the single interruptions finishing the repair of the modules. The fifth and sixth columns show the power increase achieved when moving from one repair phase to the next. The seventh column shows the power gain after the complete repair process.

Module	Pmax (W) Before repairing	Pmax (W) After repairing Twin	Pmax (W) After repairing Twin + single	ΔFase1 %	ΔFase2 %	ΔTotal %
M1	52,6	193,9	203,7	268	5	287
M2	46,8	192,7	196,3	312	2	320
M4	190,2	N/A	201,4	N/A	6	6
M5	118,0	191,0	200,8	62	5	70

Table 3
FF values measured before repair, after repairing the twin interruptions and after repairing the single interruptions and thus completely completing the repair of the modules. The percentage of FF improvement in the two repair phases is presented. The seventh column shows the FF improvement after the complete repair process.

Module	Before repairing	After repairing Twin (Phase 1)	ΔPhase1 %	After repairing Twin + single (Phase 2)	ΔPhase2 %	ΔTotal %
M1	0,61	0,68	11	0,71	5	17
M2	0,55	0,67	22	0,69	2	25
M4	0,66	N/A	N/A	0,71	7	7
M5	0,63	0,67	6	0,70	4	11

after the repair they reached values of up to 0.71.

As described in Ref. [6], a very high recovery of useful power is observed through the repair of twin interruptions, which allow a completely damaged module to produce electricity again (case of the M3 module of the cited reference) or, in less extreme cases, to multiply the power generated before the repair by up to a factor of 4 times (Phase 1). With regard to the repair of the power lost due exclusively to single interruptions (Phase 2), it has been possible to recover between 2 % and 6 % with respect to the situation of repaired twin interruptions. The complete repair process has resulted in the recovery of between 6 % and 320 % of the power. Furthermore, repairing interruptions results in a considerable improvement in FF, reaching an improvement of up to 22 % in the case of repairing twin interruptions, 7 % by repairing single interruptions with respect to the situation with twin interruptions (Phase 2) and up to 25 % if a complete repair is carried out with respect to the initial module values.

The appearance of delayed interruptions (both twin and single) leads us to suspect that there may be a line of continuity in the appearance of interruptions: It is possible that a single interruption may lead to a twin interruption in an indeterminate time period. We conclude that the repair of single interruptions is desirable, despite the modest recovery of power, for the power recovery itself and for the improvement of FF but mainly to prevent the appearance of new interruptions in the sister ribbon of a ribbon that has already suffered a fault. It is therefore recommended that when a single interruption appears, it should be repaired and, in addition, in anticipation of a future breakdown, its sister connection should be reinforced, using the same repair procedure as if it were broken.

4. Future research

It is worth noting that in this work we analyzes only modules with two ribbon. These models usually correspond to common designs manufactured more than 10 years ago. The value of this work lies in the fact that a high number of modules from this period show this type of fault.

Current market trends point out to the increase of the number of ribbons [21]. Further works will analyze the occurrence of ribbon breackages in these multiribbon layouts, and its possible reparation. From the point of view of power losses, the increase in the ribbon number will reduce the amount of power missed in case of breackage, as many ribbons should be broken to cause a high power loss. Nevertheless, aspects such as the origin of the breackages, the possibility of successive breakages of the ribbons inside the same cell once one of them has been damaged, and the effect that these breakages can have in temperature distribution or in the origin of other potential failures should be studied. One of the future activities of the authors of this work is to analyze this type of failure in a project for which funding is being sought.A benefit of repairing interruptions is that since modules with deactivated strings (i.e., with twin interruptions) disproportionately reduce module string performance and strongly reduce system performance, the cost of repairing interruptions may be worth the improvement in system performance. The data in this paper shows the positive impact of repairs on individual modules, but the added benefit of repairing under-performing module strings will likely be even greater.

One remaining task is to test the repaired modules for a long time under real conditions. This would allow the effectiveness of the repairs to be checked and the possibility of new interruptions appearing on the ribbons of the repaired modules to be monitored.

Some authors of this work are preparing a further publication in which they will analyze the economic and ecological factors allowing the commercial viability of carrying out the repair of a module with single and/or twin interruptions. In this work the environmental impact of these repairs will also be assessed. Given the length of this work, it has been considered appropriate to publish this separately. We can say that repairing a certain number of interruptions is less expensive than purchasing a new photovoltaic module of similar power to the faulty one. Therefore, in certain conditions, repairing interruptions can be economically advantageous.

5. Conclusions

This paper analyses various aspects of repairing twin interruptions and especially single interruptions in ribbons of photovoltaic modules. Its conclusions are applicable to 2-ribbon modules.

- It has been determined from EL images and alternative interruption location techniques, that single interruptions are located on the dark ribbon next to a lighted ribbon in EL images and in the part closest to the negative pole of the connection box (or of the cell itself).
- A simple, cheap and fast method has been proposed to find single interruptions, applicable to modules exposed to the sun or connected to a direct current power supply. The proposed method makes use of a magnetic compass and its results fully coincide with that of EL images and results obtained using two types of electronic current locators.
- The use of an AMR sensor has been demonstrated for the location of single interruptions, which can be used as a portable instrument in real installations under normal module operating conditions. In addition to locating single interruptions, this device allows numerical characterization of ribbon currents, as well as mapping the currents on the surface of the cells.
- Ribbon interruptions were classified into four categories: Twin interruption, Single interruption, Delayed Single interruption and Delayed Twin interruption. These categories permit progress in determining the origin and nature of ribbon interruptions in photovoltaic modules.
- An exploration of metastable interruptions was undertaken, concluding that it is advisable to locate single interruptions at various values of module current and current duration times. It is suggested to search for interruptions at 50 % of Isc and at values close to the nominal Isc. To start searching immediately at the beginning of current circulation and 15 min later. However, the location of all the metastable interruptions cannot be guaranteed.
- Ribbon interruptions in four modules were investigated, with single and twin interruptions being repaired. It was found that repairing twin interruptions recovers large values of lost power (multiples of 1/3 of the nominal power), and that repairing single interruptions recovers, in the samples analyzed, of up to 6 % more than the situation reached after repairing the twin interruptions. For the modules analyzed, repairing all interruptions increased the generated power by up to 320 %.

- It was found that, in the modules analyzed, repairing all, (twin and single) interruptions permit an improvement of up to 25 % in module fill factor.
- It is noted that the number of ribbon interruptions in failed modules can be significant. In the case of the modules analyzed in this work, the total number of ribbons repaired at the junction between cells represents 12 % of all the junctions present in the four repaired modules.
- It is recommended that all single interruptions be repaired, both in order to recover lost power and to prevent future breakdowns. In the event of a simple interruption between two cells, it is recommended to also reinforce the solder joint of the sister ribbon, to prevent a subsequent failure.

CRediT authorship contribution statement

Félix G. Rosillo: Writing – review & editing, Writing – original draft, Visualization, Supervision, Resources, Project administration, Methodology, Investigation, Conceptualization. **Maria Beatriz Nieto-Morone:** Writing – review & editing, Validation. **Richard Russell:** Writing – review & editing, Writing – original draft, Methodology. **Jesús Marín Muñoz:** Writing – review & editing, Resources, Methodology. **Juan Rodriguez Sánchez:** Resources, Methodology. **Javier Yañez Gonzalez:** Methodology. **María del Carmen Alonso-García:** Writing – review & editing, Writing – original draft, Visualization, Supervision, Resources, Project administration, Methodology, Investigation, Conceptualization.

Declaration of competing interest

The authors declare that they have no known competing financial interests or personal relationships that could have appeared to influence the work reported in this paper.

Acknowledgements

This work is part of the grant PID2020-118417RB-C21 funded by MICIN/AEI/10.13039/501100011033.

We acknowledge partial funding through MEDIDA C17.I2G: CIEMAT. Nuevas tecnologías renovables híbridas, Ministerio de Ciencia e Innovación, Componente 17 “Reforma Institucional y Fortalecimiento de las Capacidades del Sistema Nacional de Ciencia e Innovación”. Medidas del Plan de inversiones y reformas para la recuperación económica funded by the European Union – NextGenerationEU.

References

[1] S. Carrara, P. Alves Dias, B. Plazzotta, C. Pavel, Raw Materials Demand for Wind and Solar PV Technologies in the Transition towards a Decarbonised Energy System, Publications Office of the European Union, Luxembourg, 2020.
[2] Z. Ngagoum, H. Vijayakumar, S. Alpert, C. Schmid, Solar photovoltaic recycling strategies, Sol. Energy 270 (2024) 112379.
[3] G. Heath, E. Drahi, Circular economy in photovoltaics. PV P OWE R SYSTEMS T A S K 1 2. s.l., IEA PVPS, 2024.
[4] M. Nieto-Morone, F.G. Rosillo, M.A. Muñoz-García, M.C. Alonso-García, Enhancing photovoltaic module sustainability: defect analysis on partially repaired modules from Spanish PV plants, J. Clean. Prod. 461 (2024) 142575.
[5] M. Köntges, S. Kurtz, C.E. Packard, J. Ulrike, K.A. Berger, K. Kato, F. Thomas, H. Liu, V. Iseghem, Review of Failures of Photovoltaic Modules. s.L., INTERNATIONAL ENERGY AGENCY, 2014.
[6] F.G. Rosillo, M. Nieto-Morone, J. Benavides, F. Soriano, S. Temprano, C. González, M.C. Alonso-García, Repairing ribbon bus bar interruptions in photovoltaic modules using non-intrusive interruption location, Renew. Energy 223 (2024).
[7] Y. Kawano, J. Chantana, Y. Kuroda, K. Hirose, T. Minemoto, Development of repairing technique for interconnection of silicon photovoltaic modules using an induction heating system, Sol. Energy 261 (2023) 55–62.
[8] E Annigoni, A Virtuani, J Levrat, et al., Quantifying and modeling the impact of interconnection failures on the electrical performance of crystalline silicon photovoltaic modules, Prog Photovolt Res Appl 27 (2019) 424–432.
[9] Dylan J. Colvin, Eric J. Schneller, Kristopher O. Davis, Impact of interconnection failure on photovoltaic module performance, Progress in Photovoltaics 29 (5) (2021) 524–532.
[10] J. Walzberg, A. Carpenter, G.A. Heath, Role of the social factors in success of solar photovoltaic reuse and recycle programmes, Nat. Energy 6 (2021) 913–924.
[11] K. Tada, S. Kawamoto, N. Yamada, T. Kimura, M. Iwahashi, T. Tadaumi, K. Kato, Sensor Placement Optimization in On-Site Photovoltaic Module Inspection Robot for Fast and Robust Failure Detection, IEEE 42nd Photovoltaic Specialist Conference (PVSC). Proceedings Paper, New Orleans, Louisiana, USA : s.n, 2015.
[12] D. Lausch, M. Patzold, M. Rudolph, C. Lin, J. Froebel, K. Kaufmann, Magnetic Field Imaging (MFI) of Solar Modules, 35th EU PVSEC, Brussels, Belgium : s.n, 2018.
[13] R. Alfanz, Y. Okazaki, T. Ikegami, Y. Deng, Integrated micro tesla magnetic sensor for detecting photovoltaic cells failure, IOP Conf. Ser. Mater. Sci. Eng. 673 (2019) 012052.
[14] Honeywell. [Online] https://aerospace.honeywell.com/content/dam/aerobt/en/documents/learn/products/sensors/datasheet/N61-2056-000-000_MagneticSensors_HMC-ds.pdf.
[15] F.G. Rosillo, J. Yañez, M.C. Alonso, Marín, J. *P202430974* Spain, 2024.
[16] National high magnetic field laboratory [Online] February, https://www.youtube.com/watch?v=RwilgsQ9xaM, 2017.
[17] A. Rocky, M. Burhanzoi, O. Kenta, T. Ikegami, S. Kawai, Photovoltaic module fault detection using integrated magnetic sensors, IEEE J. Photovoltaics 9 (6) (2019). NOVEMBER 2019.
[18] U. Zeller, L. Dominik, P. Matthias, K. Kai, S. Slaby, S. Schoenfelder, Comparison of magnetic field imaging (MFI) and magnetic field simulation of silicon solar cells, AIP Conf. Proc. (2019) 2147.
[19] K. Buehler, K. Kaufmann, M. Patzold, M. Sprenger, S. Schoenfelder, Identifying defects on solar cells using magnetic field measurements and artificial intelligence trained by a finite-element-model, EPJ Photovoltaics 14 (2023) 12.
[20] A. Tummalieh, M. Mittag, J. Weber, D. Yucebas, L. Schäfer, R. Quay, R. Reichel, H. Neuhaus, Impact of string connection and contact defects on electrical current distribution in solar cells and modules: a model validated by magnetic field imaging, Prog. Photovoltaics Res. Appl. 33 (2025) 219–235.
[21] M. Fischer, M. Woodhouse, P. Baliozian, International Technology Roadmap for Photovoltaics (ITRPV), VDMA e. V. Photovoltaics Equipment, Frankfurt am Main, 2024.